Journal of Visualization, Vol. 3, No. 2 (2000) 195-202

Particle Imaging Sizing: GLMT Simulations

Girasole, T.*, Ren, K. F.*, Lebrun, D.*, Gouesbet, G.* and Gréhan, G.*

* UMR 6614/CORIA, CNRS-Université et INSA de Rouen, 76 130 Mont-Saint-Aignan, France.

Received 21 September 1999.
Revised 15 October 1999.

***Abstract*:** Defocused off-axis images of particles are computed in the framework of the generalized Lorenz-Mie theory. Two exemplifying cases are studied: interferometric sizing at large off-axis angles and imaging in near forward directions (shadow Doppler velocimetry).

***Keywords*:** Lorenz-Mie theory, imaging diffraction.

1. Introduction

In the field of spray analysis, a large number of techniques has been developed to measure the properties of droplets. The most often measured properties are the velocity and the size of the droplets. These measurement techniques can be sorted in two categories: (i) point measurement techniques which measure droplets one after one, waiting that the droplets cross a small optical probe, (ii) integral methods which simultaneously probe an ensemble of particles in a large control volume. Nowadays, the most popular techniques for velocity measurements are LDV and PIV. LDV measures the velocity of individual particles while PIV[1], [2], [3] measures velocities of a lot of particles in a plane, giving 2D velocity maps. PDA is an extension of LDV which gives the possibility to measure at the same time the velocity and size of individual particles.[4], [5], [6] Imaging techniques are a natural potential of these approaches as interferometric imaging for PIV and shadow Doppler for LDV.

Imaging techniques can be sorted as on-axis and off-axis imaging. On-axis imaging of droplets, including defocusing effects, have been extensively explored in the framework of Lorenz-Mie theory (plane wave)[7] and of generalized Lorenz-Mie theory (incident Gaussian beam).[8], [9], [10] This rigorous approach has also been applied to cylindrical scatterers.[11] For off-axis imaging, only the case of in focus particles has been investigated.[10] This paper is then devoted to the analysis of off-axis defocused images of spherical droplets. Two complementary cases must be studied corresponding to two techniques under development (i) one incident beam with a large axis angle of collection (ii) two incident beams with a near forward off-axis collection.

The paper is organized as follows. Section 2 is devoted to interferometric imaging. Subsection 2.1 recalls the theoretical basis of off-axis imaging. Subsection 2.2 compiles numerical predictions, devoted to the defocusing effect. Section 3 is devoted to shadow Doppler velocimetry. Section 4 is a conclusion.

2. Interferometric Imaging

2.1 Theoretical Background

On-axis and off-axis imaging of spherical particles is strongly connected with glare points. This section is then organized into three subsections. The first subsection recalls the glare point theoretical background. The second subsection discusses the interest of defocus off-axis imaging, and the last one describes a numerical scheme.

2.1.1 Glare points and off-axis imaging

According to van de Hulst,[12] glare points are bright spots seen on the surface of a water drop when it is illuminated by a broad parallel beam and viewed under an arbitrary scattering angle. These bright spots can be computed from Lorenz-Mie theory by carrying out a Fourier integral on the aperture of the collecting lens. These computations describe the distribution of energy in the image plane. In the geometrical optics framework, the bright spots can be, for most of them, interpreted as created by a particular class of rays but not all of them.[12], [13] For example, in forward direction, they are created by the light externally reflected and the light directly refracted through the particle ($p=0$ and $p=1$ rays, according to van de Hulst notation). Then, in the image plane, at least two bright spots appear on one particle for an arbitrary scattering angle.[10] The direct measurement of the bright spots can be used to measure particle diameter and particle refractive index. Nevertheless, the magnification required to measure the glare spots must be so large that its use is not easy in realistic multiphase flows. An indirect use of the glare spots is described in the next subsection.

2.1.2 Off-axis defocused imaging

Starting from the work of Anders et al.,[14] who demonstrated that a phase difference for each class of rays is given by a simple relation, Glover et al.[15] have established that the angular fringe separation $\Delta\theta_m$, in the image, is directly dependent on the particle size:

$$\Delta\theta_m = \frac{2\pi}{\alpha\left(1+\frac{1}{m}\right)} \tag{1}$$

where m is the relative refractive index of the particle and α is the size parameter defined by $\alpha=\pi d/\lambda$. d is the particle diameter and λ is the wavelength of the incident light.

2.1.3 Numerical scheme

Figure 1 displays the scheme of the computational geometry. The incident beam displays a finite angle with respect to the optical axis. A relay lens forms an image of the object plane on an image plane. The recording element (photographic plate or CCD) is in a plane located at a distance l_i of the image plane. When l_i is negative, the recording element plane is between the lens and the image plane.

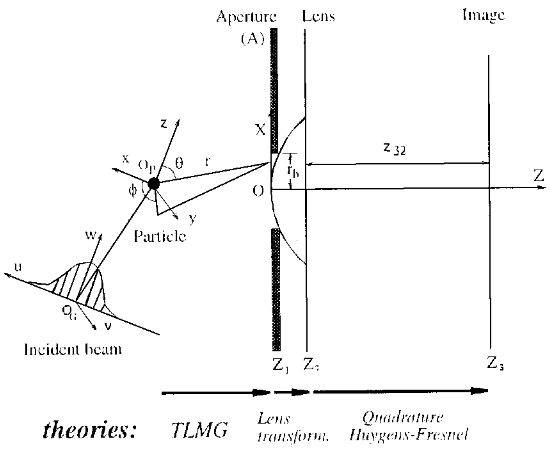

Fig. 1. Scheme of GLMT image computations.

We simulate this configuration as follows (i) the light propagation from the particle to the input plane of the lens is computed by GLMT, (ii) the propagation of the light from the input plane (Z_1) to the output plane (Z_2) of the lens (assumed to be a perfect phase lens) is described by only introducing a phase shift,[16] (iii) the propagation of the light from the output plane of the lens (Z_2) to the detector plane (Z_3) is computed by a Huygens-Fresnel integral. This integration is carried out using Hopkins' approach.[17], [18]

2.2 Exemplifying Numerical Results

Computations are carried out for various apertures, magnifications, particle sizes and particle locations.

2.2.1 Effect of the defocus

First, we assume that the scatterer is a water droplet, with a refractive index of 1.33-0i. The scattering angle is set of 66.5° with the electric polarization of the incident beam perpendicular to the observation plane, implying the same intensity for the reflected and the refracted lights

The first study is devoted to dependence of the light intensity in the detector plane versus the value of the defocus. The focal length is 600 mm and the lens diameter is 100 mm, corresponding to an aperture number equal to 6. The first series of computations is carried out for a magnification equal to 5 (the distance between the object plane and the lens is equal to 0.72 m while the distance between the lens and the image plane is 3.6 m).

Figure 2 (default=0) displays the intensity distribution when the detector plane is located at the image plane. The abscissa unit is the distance on the image plane divided by the particle size. The distribution of intensity is here characterized by two spots of high intensity, corresponding to the glare spots. One of the spots is created by the reflected light while the other is created by the refracted light. In arbitrary unit, the mean intensity of these peaks is about 30. Next, the detector plane is moved away from both the lens and the image plane. The series of figures displays the light distribution versus the value of the defocus. The size of the images increases with the defocus distance (Fig. 3) while the number of fringes is nearly constant when the defocus is big enough (see Fig. 4). Furthermore, the mean intensity sharply decreases with the distance (see Fig. 5).

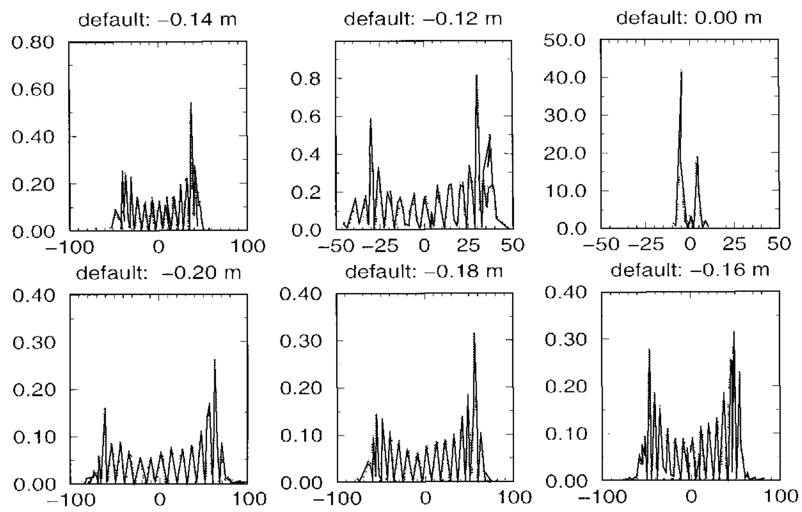

Fig. 2. Example of the evolution of the image with the defocus. The particle is a water droplet (m=1.33) with

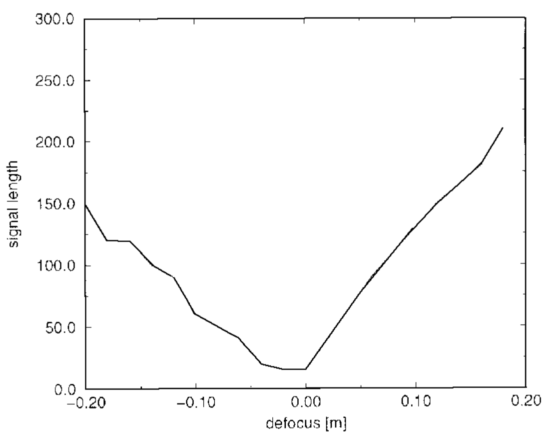

Fig. 3. Image size versus the defocus length.

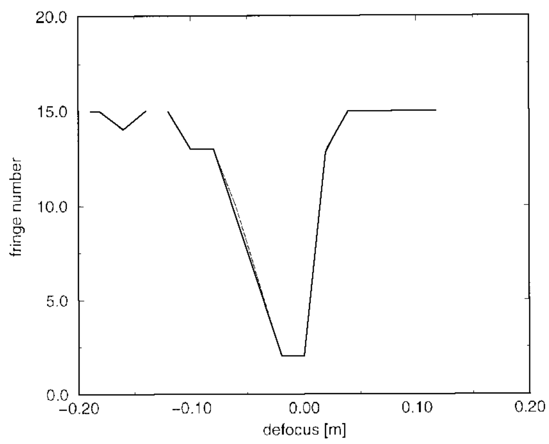

Fig. 4. Fringes number versus the defocus length.

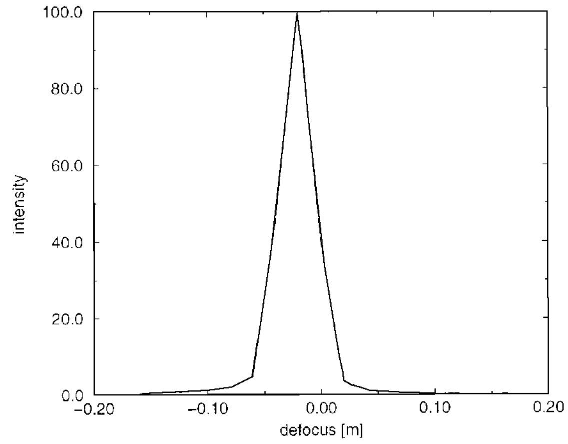

Fig. 5. Image maximum intensity versus the defocus length.

2.2.2 Size dependence

Next, for the same lens, the same magnification and a distance between the object plane and the lens equal to 0.72 m while the distance between the lens and the detector plane is 3.4 m, the distribution of light is displayed in the series of Fig. 6 with the particle size d as a parameter. The images exhibit a good visibility. Figure 7 exemplifies a close linearity relating the number of fringes and the particle diameter for this geometry.

3. Shadow Doppler Velocimeter

The Shadow Doppler Velocimeter has been developed to measure the size of irregular particles. Basically it consists in imaging the control volume of a laser Doppler anemometer with a linear CCD camera. The dimension and shape of irregular scatterers (more precisely of their projection) are reconstructed from a time series of slices realized with the linear camera.

The computational scheme is essentially the same than the one introduced previously. Nevertheless, the numerical difficulties are more important because we must now compute and add four contributions to obtain an image (i) the field from beam 1 (ii) the field from beam 2 (iii) the field scattered by the particule from beam 1 (iv) the field scattered by the particle from beam 2.

The angle between the two beam is set to 2.86°, the wavelength is 0.488 μm, and the collecting lens has a diameter equal to 10 cm with a focal length equal to 600 mm. Systematic computations have been carried out. The particle diameter ranges from 10 to 160 μm, by steps of 50 μm. Two examples of results are given here. First, Figure 8 compares the images of a 10 μm droplet when the relative intensity between the two incident laser beams varies from 1 to 0.1.

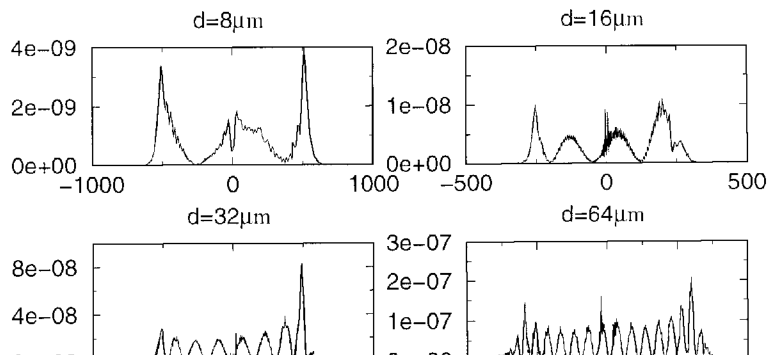

Fig. 6. Out of focus images for different particle sizes (8, 16, 32 and 64 μm).

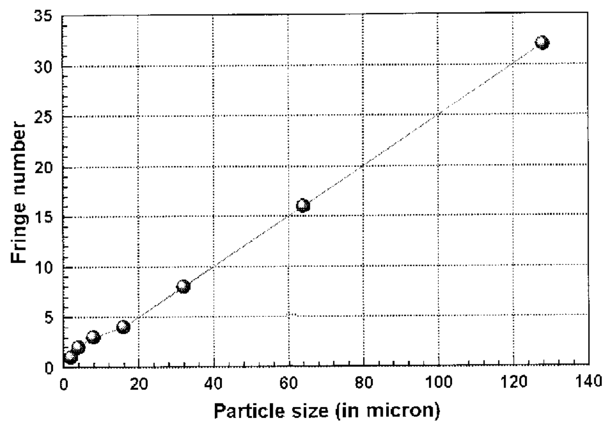

Fig. 7. Number of fringes versus the particle size.

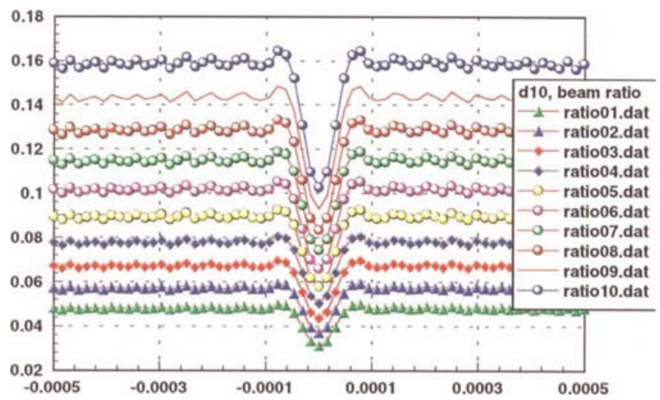

Fig. 8. Evolution of the contrast of the image of a 10 μm droplet with the relative intensity of the two laser beams as parameter.

Next, Figure 9 displays the behaviour of the contrast for a 10 μm droplet. The droplet is located along the optical probe axis, the geometrical optic in-focus location is predicted at 0. The step between two location of the droplet is 50 μm. The shadow as well as the focusing effects are emphasized on this figure, but the best image location is find to be at about 1000 microns

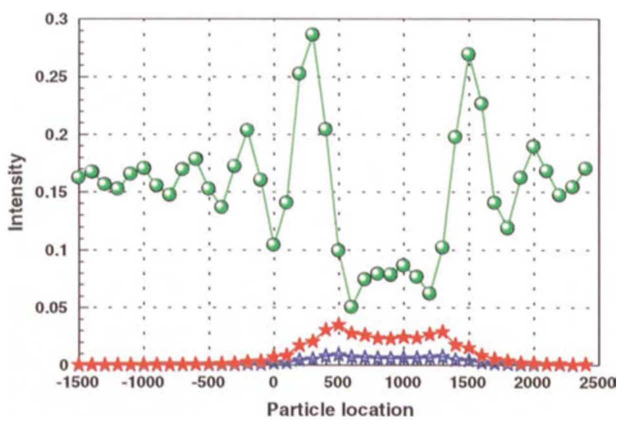

Fig. 9. Evolution of the contrast for a 10 μm droplet located along the optical probe axis.

To explore the origine of this effect, maps of intensity and phase on the input surface of the lens has been computed for a 40 μm water droplet on which impinges a large beam (W_0=1.5 mm) and for 3 particle locations: −1100, 0 and +1100 μm. Only one map of intensity is displayed in Fig. 10, because the intensity distribution is equal for the three particle locations. Then the iso-phase level are displayed in Figs. 11 to 13 for a particle location of −1100, 0 and +1100 μm. For the phase, large differences are predicted. This effect correspond to have an effective focal lens which is a function of the angle of the two direct beams relatively to the input surface of the imaging lens.

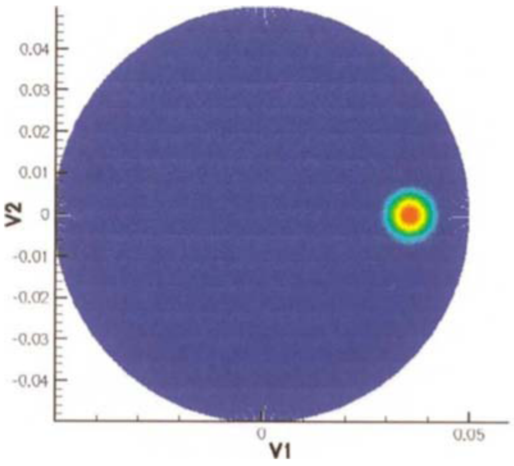

Fig. 10. Iso-level of scattered intensity.

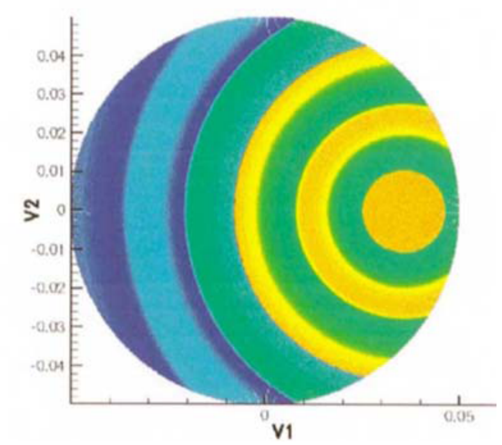

Fig. 11. Behaviour of the phase on the input surface of the lens for a 40 μm diameter droplet. The parameter is the particle location in the control volume (−1100 μm).

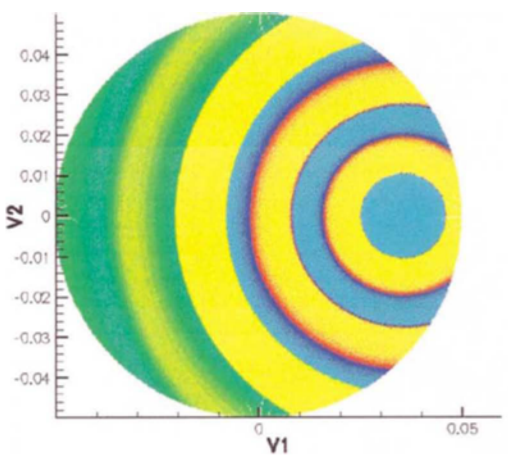

Fig. 12. Behaviour of the phase on the input surface of the lens for a 40 μm diameter droplet. The parameter is the particle location in the control volume (0 μm).

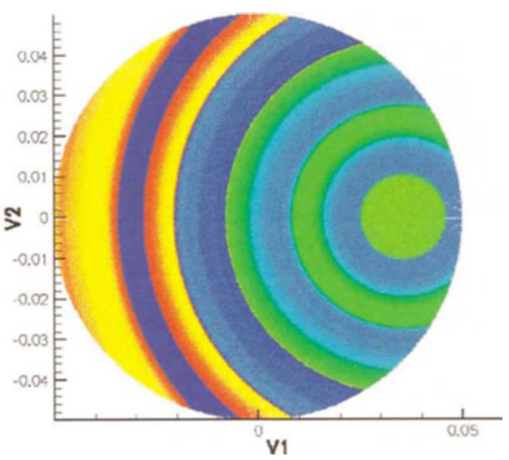

Fig. 13. Behaviour of the phase on the input surface of the lens for a 40 μm diameter droplet. The parameter is the particle location in the control volume (+1100 μm).

4. Conclusion

The generalized Lorenz-Mie theory is used in connection with classical Fresnel-Huygens integral to compute the properties of the light scattered by spherical scatterers which are off-axis and out-of-focus. This approach gives the possibility to compute libraries of images with very well mastered geometric and optical conditions. These libraries of images can be used to understand some particular situations and/or to test various signal processing schemes in order to extend the potential of imaging measurement techniques.

References

[1] Adrian, R. J., Multi-point optical measurements of simultaneous vectors in unsteady flow — a review. Int. J. Heat and Fluid Flow, 7, 2, (1986), 127-145.

[2] Prasad, A. K. and Adrian, R. J., Stereoscopic particle image velocimetry applied to liquid flows. In Six International Symposium on application of laser techniques to fluid mechanics, 20-23 July, Lisbon, Portugal (1992), 6-1-1.6-1-8.

[3] Lecordier, B., Mouqallid, M., Vottier, S., Rouland, E., Allano, D. and Trinité, M., CCD recording method for cross-correlation piv development in unstationary high speed flow. Experiments in Fluids, (1994).

[4] Durst, F. and Zaré, M., Laser Doppler measurements in two phase flows. In Proceedings of LDA-Symposium, Copenhagen (1975), 403-429.

[5] Saffman, M., Buchhave, P. and Tanger, H., Simultaneous measurement of size, concentration and velocity of spherical particles by a laser Doppler method. In Laser Anemometry in Fluid Mechanics-II, Ed: Adrian, Durao, Durst, Mishina and Whitelaw, LADOAN-Lisbon (1984), 85-104.

[6] Bachalo, W. D. and Houser, M. J., Phase/Doppler spray analyzer for simultaneous measurements of drop size and velocity distributions. Optical Engineering, 23, (1984), 583-590.

[7] Schaub, S. A., Alexander, D. R. and Barton, J. P., Theoretical model for the image formed by a spherical particle in a coherent imaging system: comparison to experiment. Opt. Eng., (1989), 565-571.

[8] Schaub, S. A., Alexander, D. R., Barton, J. P. and Emanuel, M.A., Laser beam interaction with methanol droplets: effects of relative beam diameter. Appl. Opt., 28, 9, (1989), 1666-1669.

[9] Lebrun, D., Touil, C. E. and Özkul, C., Methods for the deconvolution of defocused-images pairs recorded separately on two CCD cameras: application to particle sizing. Appl. Opt., 35, 32, (1996), 6375-6381.

[10] Ren, K. F., Lebrun, D., Özkul, C., Kleitz, A., Gouesbet, G. and Gréhan, G., On the measurement of particles by imaging methods: theoretical and experimental aspects. Part. Part. Syst. Charact., 13, (1996), 156-164.

[11] Lebrun, D., Belaid, S., Özkul, C., Ren, K. F. and Gréhan, G., Enhancement of wire diameter measurements: comparison between Fraunhofer diffraction and Lorenz-Mie theory. Opt. Eng., 35, 4, (1996), 946-950.

[12] Van de Hulst, H. C. and Wang, R. T., Glare points. Applied Optics, 30, 33, (1991), 4755-4763.

[13] Lock, J. A. and Woodruff, J. R., Non-Debye enhancement in the Mie scattering of light from a single water droplet. Appl. Opt., 28, 3, (1989), 523-529.

[14] Hesselbacher, K. H., Anders, K. and Frohn, A., Experimental investigation of Gaussian beam effects on the accuracy of a droplet sizing method. Applied Optics, 30, 33, (1991), 4930-4935.

[15] Glover, A. R., Skippon, S. M. and Boyle, R.D., Interferometric laser imaging for droplet sizing: a method for droplet-size measurement in sparse spray systems. Applied Optics, 34, 36, (1995), 8409-8421.

[16] Goodman, J. M., Introduction à l'optique de Fourrier et à l'Holographie. (1972) Traduit par C. Durou et J.P. Pérez de: Introduction to Fourier Optics (1968), McGraw Hill Company, New York.

[17] Stamnes, J. J., Wave in focal regions (1986)

[18] Hopkins, H. H., The numerical evaluation of the frequency response of optical systems. Proc. Phys. Soc. B., 70, (1957), 1002-1005.

Author Profile

Thierry Girasole: He received his Ph.D. in Physics in 1991 from the University of Rouen. He worked in the thermal instabilities in multiphase flows during his Ph.D. After the Ph.D. he worked as an engineer into the UMR 6614 CNRS in the area of light scattering topics. His research interests generalized Lorenz Mie theories and their applications in laser-based techniques as phase Doppler analyser or imagery, as well as 4 Flux and Monte Carlo methods applied to multiple scattering.

Kuan Fang Ren: He obtained a MSc degree in radiophysics in 1988 from Northwest Telecommunication Engineering Institute, China, and a Doctorat ès Sciences in 1995 from the University of Rouen. Since 1998, he is a Maître de Conférence (Assistant professor) at Rouen University. His research interests include scattering of finite laser beams by homogeneous or inhomogeneous particles and its applications in particle sizing techniques such as particle imaging, rainbow, phase Doppler anemometry, turbidimetry, etc.

Denis Lebrun: He received his PhD degree in optoelectronics from the University of Rouen University, France in 1992. Since 1993, he is a Maître de Conférence (Assistant professor) at Rouen University. His current research interests include image and signal processing, digital and optical wavelet transforms, liquid crystal spatial light modulators, diffraction phenomena and holography.

Gérard Gouesbet: He recieved his third cycle thesis in 1973 and his state thesis in 1977. He has been a researcher of the French National Center of Scientific Research from 1975 to 1983 and since then he is a professor at the National Institute of Applied Sciences of Rouen where he is heading a laboratory of about 35 persons (the LESP). He is honorary professor of Xi-Dian University, of the North-Eastern Liaoming University, in China, and a member of the New York Academy of Sciences. His research interests included the modelling of two-phase flows, light scattering theories and applications, instabilities and non linear dynamics.

Gérard Gréhan: He received his third cycle thesis in 1980 and his state thesis in 1985 both from University of Rouen. He is a researcher of the French National Center of Scientific Research (CNRS) since 1980 where he has actually a position of Directeur de Recherche. He is honorary professor of Xi-Dian University, China. His research interest meanly interaction between laser beams and particle, including theoretical, numerical as well as experimental approaches. A particular interest is devoted to optical metrology (imaging, optical tweezers, PDA, ...).